CORROSION/2002 Paper #02259

# Modeling and Measurements of Cathodic Prevention Distribution in Partially Submerged Reinforced Concrete

Francisco J. Presuel, S.C. Kranc, Alberto A. Sagüés
Dept. of Civil and Environmental Engineering
University of South Florida
Tampa, FL, 33620

## ABSTRACT

Cathodic prevention was implemented with commercial Zn bulk anodes on laboratory columns simulating a reinforced concrete marine system. Two computational models of these laboratory columns were implemented. The results obtained from both models were in reasonable agreement with the experimental observations. One of the models was used to predict cathodic prevention throwing power on field scale structures, as a step towards field application. These predictions suggest that with an immersed anode useful levels of cathodic prevention may be reasonably expected, even under conservative assumptions, in the area immediately above high tide where conditions are otherwise very severe.

Keywords: Cathodic Prevention, Numerical Modeling

## INTRODUCTION

Cathodic protection (CP), implemented either as an impressed current or as a sacrificial anode system, has been successfully used to mitigate corrosion on reinforced concrete structures. One relatively recent variation of the CP technique is cathodic prevention (CPrev) [1 – 7] for new reinforced concrete structures. To date, CPrev has been principally used to protect atmospherically exposed structures (e.g., bridge decks), by means of impressed current systems [1-6]

CPrev delays the onset of corrosion by polarizing the still passive steel reinforcement to a more negative potential at which corrosion is less likely to initiate. Additional benefits may accrue by slowing the migration of chloride ions toward the rebar and by increasing $OH^-$ concentration at the rebar surface. Although this technique requires a system similar to that used for CP, in contrast to CP, CPrev is usually applied early in the service life of the structure, before the initiation of corrosion. Thus, the system is usually installed during the construction of a structure, and energized a short time later. Since the rebars are in a passive state, the

required applied current is much smaller than that normally needed for CP. Cathodic polarization by approximately 100 mV is said to increase the chloride threshold for initiation of corrosion by as much as an order of magnitude [1-2]. More recent publications [8-12], based on experiments conducted in reinforced concrete or mortar cells, suggest that cathodically polarizing the steel from –100 to -200 mV (SCE) increases the chloride threshold by at least 1.5 to 3 times.

CPrev may be an attractive method to protect new marine reinforced concrete substructures (MRCS) using simple sacrificial submerged anodes, which are economical and easy to replace. The portion above water (AW) may be more protected than in conventional CP because of the lower current demand. It is therefore of interest to find how high above water sacrificial submerged anodes may be able to provide CPrev in these systems.

A literature search found only one published work to date reporting the use of CPrev on a partially submerged structure with sacrificial submerged anodes [2]. In that investigation, only the bottom fifth of a 1 m high laboratory specimen was submerged in artificial seawater, but the whole specimen was found to be cathodically polarized 100 mV or more. These results were encouraging but the test system had not been thoroughly characterized. Additional investigation beyond this limited experiment is needed, and computer modeling offers a powerful means for this evaluation.

In the present investigation, both a CPrev experimental installation and computer models of corrosion distribution in reinforced concrete were utilized to evaluate the extent of CPrev for partially submerged piles provided by a bulk sacrificial anode placed below water. The experiments were made on laboratory columns that were available from an ongoing investigation. For the computational models, a pile was assumed to be at the beginning of its service life, with passive rebar. The models used as input parameters the concrete electrical resistivity, oxygen diffusivity (one model version only), and the cathodic polarization parameters and iron dissolution rate at the passive rebar, obtained from experimental measurements or from values reported in the literature. The experimental and model results describe the state of the system after connection of a zinc sacrificial anode. These results are used to gain insight as to what throwing power above water can be achieved.

## EXPERIMENTAL

### Experimental Arrangement

Four existing reinforced concrete columns were tested (Figure 1) [13]. Each column had 11 horizontal rebar segments, each segment with an exposed surface area of 166 $cm^2$. The segments were numbered starting from #1 at the top of the column. Only segments #1 to #8 (or #1 to #9 depending on the column), which were in the passive condition, were used for these experiments. The remaining lower segments were in the active condition and were kept isolated. Electrical connections to all segments and embedded reference electrodes [14] were routed to a switch box. The switches kept the segments to be used normally interconnected. During the experiments sacrificial zinc bulk anodes were connected to the passive rebar segment assembly and the extent of cathodic polarization of those segments was determined.

The rebars were commercial #7 stock made of plain carbon steel (0.23 % C) and as-received had a high temperature mill scale. The rebars were intentionally pre-rusted by dipping in a 3.5% NaCl solution. The concrete had a water-cement ratio of 0.45, 360 $kg/m^3$ Type I Portland

cement, and sand as fine aggregate. The coarse aggregate was limestone with maximum size of 1 cm. The concrete mix for the lower 25.4 cm of each column had 11.9 kg/m$^3$ $Cl^-$ added, by including the appropiate amount of NaCl. Since construction, 9 ½ years before these tests, the columns were placed in a tank with the lower 12.6 cm submerged in salt water (5% NaCl solution). The average temperature and relative humidity (RH) were 21.5°C ± 2°C and 60 % ± 15% respectively in the laboratory during the time that the CPrev system was in place. Two of the columns (named Set W) had been subject to periods of fresh water wetting in the past and retained overall lower resistivity than the other two columns (named Set D). Figure 2 shows typical concrete resistivities as a function of elevation, obtained with a.c. measurements described elsewhere [15].

The rebar static potential measured against the embedded reference electrodes, inter-rebar segment current and inter-rebar segment concrete resistivity were monitored before and during the application of CPrev. The rebar static potential was converted to the saturated calomel electrode (SCE) scale by periodically calibrating the embedded reference electrodes vs. a SCE. All reported potential values are referred to SCE scale. Also, all potentials are presented corrected for ohmic potential drop (obtained using information from periodic instant-off measurements). The current density delivered by the anode to each of the rebars segments was calculated from the inter-rebar segment current measurements and accounting for the rebar surface area. A depolarization test was conducted after CPrev had been applied for 120 days. The depolarization test consisted of disconnecting the anode and opening all switches at the same time then registering the subsequent evolution with time (up to ~22 hrs) of each rebar segment potential with respect to its corresponding embedded reference electrode. Net depolarization values were reported as the difference between the instant-off potential (just after disconnection) and the potentials measured subsequently during the rest of the test.

The CPrev test was preceded by a conditioning period, in which it was determined that the top 8 and 9 segments were passive on column sets W and D respectively [15]. Also during the conditioning period the interconnected passive segments were allowed to develop steady conditions for at least 100 days after isolation of the active segments. Just before the beginning of CPrev the potentials of the passive rebar segments ranged from –35 mV to 10 mV. There was less than 10 mV difference from the top to the bottom passive rebar segment in any given column, and on all these segments the net current density was less than 0.001 μA/cm$^2$. To start CPrev application four commercial Zn bulk anodes (one per column) were placed in the water and then separately connected to the passive rebar assembly of each column.

**Experimental Results**

Upon connection of the anode to the passive rebar segments (Day 0), there was a brief (~1 day) transient period after which relatively steady conditions developed. The anode connection resulted in cathodic polarization of the rebar segments (especially pronounced at the lower rebar segments). The potential and current densities measured at each rebar segment varied moderately with time, likely reflecting variations in the concrete resistivity due to changes on the degree of water saturation of the concrete as the room RH varied.

Potential and Current Delivery of Anodes. Figure 3 shows the average instant off potential values and the average current delivered by the anodes over time, grouped by column type over time. The average anode potential values were ~ –1020 mV with currents on the order of 1 mA, as expected from commercial Zn anodes of this type.

Currents Density Delivered by the Anodes to each Rebar Segment. Figure 4 shows the cathodic current densities delivered to each rebar segment during the first 305 days of CPrev aplication on column W1. Similar trends with time were observed in the other three columns. The bottom three rebar segments in all columns received at least 0.1 $\mu A/cm^2$, and the lower segment as much as ~5 $\mu A/cm^2$. The five upper rebar segments on columns of Set W received about one order of magnitude larger current density than the corresponding rebar segments in Set D. Average values for both sets are shown later in Figure 10.

Potential Values of Rebar Segments During Cprev. The average and range of potentials for each rebar segment are shown in Figure 8 (grouped per column set). Pairs of corresponding rebar segments (e.g. #1 segments in Set W) had very similar average potentials, typically within 15 mV of each other.

Polarization. Polarization is defined here as the downward steady state potential shift of each rebar segment, corrected for ohmic potential drop, resulting from anode connection. Table 1 shows the results for each of the four columns obtained by averaging over the first 305 days of CPrev application, but excluding the first day transient. All the rebar segments in the W columns were polarized by at least 100 mV by the Zn bulk anode. This performance is significant considering that concrete resistivity measured was substantial (>70 k$\Omega$-cm above 60 cm elevation) at the upper levels. Polarization > 100 mV in columns of Set D only reached up to rebar segment #6 (60 cm elevation), but concrete resistivity was already 500 k$\Omega$-cm at that elevation. From Figures 9 and 10 it can be observed that the current density required to obtain 100 mV polarization was ~ 0.01 $\mu A/cm^2$, confirming the very low current demand for CPrev. This also agrees with the results presented in the following section.

Polarization Curve – E-log i Curve. The rebar potentials and the net current densitiy values for all the rebar segments measured at day 80 with CPrev were used to build an E-log i graph, Figure 5. The shape of the plot suggests that most of the segments were under cathodic activation polarization, and cathodic polarization parameters can be calculated from the data shown on this figure. The line fitted through the straight portion of the plotted data by regression analysis, indicates a cathodic Tafel slope $\beta_c$ ~ 145 mV/decade. The magnitude of the passive rate of dissolution $i_p$ was estimated by assuming that the plateau apparent near ~-45 mV in Figure 5 corresponds to a condition approaching zero net current, i.e. where the passive current density $i_p$ equals that for oxygen reduction at that potential. This assumption is supported by the observation that the open circuit potential (OCP) of steel in concrete is typically ~0 mV to -100 mV [16,17], roughly the same as that of the upper segments of the columns examined here. Thus simple Tafel extrapolation of the cathodic current to the point where potential ~-45 mV in Figures 5 indicates $i_p \sim 2.5x\ 10^{-3}\ \mu A/cm^2$. The values of the oxygen reduction exchange current density and effective equilibrium potential ($i_{OC}$ and $E_{OC}$ respectively) are not known individually, but if one of them is arbitrarily chosen the other can be defined so that any resulting segment potential-current density pair falls along the Tafel line. For convenience a nominal value of $E_{OC}$ = 100 mV was chosen, which resulted in a nominal value of $i_{OC}=2.5x10^{-4}\ \mu A/cm^2$.

Depolarization Test. Figure 6 and 7 show net depolarization curves for the rebar segments of columns W1 and D1. Very similar curves were observed on columns W2 and D2 respectively. The lowest segment in the D columns (#9) was in a zone of very moist concrete. The initial depolarization of segment #9 was much slower than for segment #8 in the same columns, likely as a result of slow oxygen transport through the wet concrete. This observation

suggests that there was a significant component of concentration polarization in segment # 9, also supported by the large deviation from apparent Tafel behavior observed for that segment in Figure 5.

Polarization vs Net Depolarization. The observed net depolarization after 22 hours was in average 53% of the separately determined polarization. This behavior is not surprising in view of previous reports [18] that the depolarization of steel in concrete obtained after 4 hours can be as little as 25% of the total polarization.

## MODELING

Two modeling approaches were implemented: a three-dimensional (3-D) model, which handled combined activation concentration polarization cathodic behavior and a simplified one-dimensional (1-D) model. The 3-D model replicated the geometry of the laboratory column and was computationally demanding, whereas the 1-D model required less resources.

### 3-D Model Description

A brief description of the 3-D model is presented in this section and includes the model governing equations, boundary conditions, model inputs and outputs, and the solution strategy. This model is a modification of previous work described in detail elsewhere [19-20].

a) Governing equations. The concrete was treated as a homogeneous medium, but with both concrete resisitivity and oxygen diffusivity varying on the vertical direction.

The current density in the bulk of the concrete (termed i) was calculated by

$$i = \rho^{-1} \nabla E \qquad (1)$$

where $\rho$ concrete resistivity, E=potential in concrete. The potential and the concentration of oxygen in the bulk of the concrete obeyed charge and mass concentration requirements:

$$\nabla(\rho^{-1}\nabla E)=0 \qquad (2)$$

$$\nabla(D_o \nabla C)=0 \qquad (3)$$

where $D_o$=Oxygen diffusivity, C=Oxygen concentration

b) Boundary conditions. The oxygen flow on the steel surface was related to the cathodic current density by Faraday's Law:

$$i_c = 4FD_o \frac{\partial C}{\partial n} \qquad (4)$$

where n=normal direction to the rebar surface, F=Faraday constant. On the surface of the concrete the oxygen concentration was assumed to be constant. It was assumed that at the ends of the column there was no oxygen transport. At the rebar, the iron dissolution reaction

was assumed to proceed at a small and constant rate described by the anodic passive current density $i_p$. Oxygen reduction was assumed to follow Butler-Volmer kinetics as suggested in part by the Tafel behavior in Figure 5:

$$i_c = i_{oc} \frac{C}{Co} e^{(E-E_{OC})/\beta_c} \qquad (5)$$

where Co=effective oxygen concentration of concrete in direct contact and equilibrium with air, $\beta_c$ = cathodic Tafel slope. The reverse reaction is ignored because the system is always far below the oxygen redox potential.

Above the water line the current flow through the outer concrete surface was set to zero. The surface of the concrete submerged in 5% NaCl solution was assumed to be equipotential. As the resistivity value of 5% NaCl solution ($\rho \sim 20\ \Omega$-cm) is much smaller than those assumed for the concrete, the assumption of an equipotential concrete-solution interface was considered to be a justifiable approximation.

c) Model inputs. The model inputs are: concrete properties (resistivity and an oxygen diffusivity as function of elevation), values for the electrochemical polarization parameters, and values for the constant boundary conditions (oxygen concentration at the surface of the concrete and the equipotential value for the submerged portion of the column). The resistivity profiles used for the model were based on the measured resistivities presented in Figure 2.

The values for polarization parameters used in the model were based on the experiment results (E-log i analysis): $i_{OC} = 2.5 \times 10^{-4}$ $\mu A/cm^2$, $E_{OC}$=100 mV, $\beta_c$ =145 mV/decade and $i_p = 2.5 \times 10^{-3}$ $\mu A/cm^2$. A value of –1020 mV was used as a nominal working anode potential. The effective concentration of $O_2$ was expressed in moles of $O_2$ per $cm^3$ of pore water in concrete. Thus, the concentration of $O_2$ (Cs) at the concrete surface was set to $Cs=3 \times 10^{-7}$ moles/$cm^3$ (atmospheric conditions [21]). The values of $D_o$ were chosen as indicated in reference [19], modified as follows: For regions below the water line $D_o=6 \times 10^{-6}$ $cm^2$/sec. When $\rho$ > 60 kW-cm, $D_o = 6 \times 10^{-4}$ $cm^2$/sec. For portions in between, $D_o$ was obtained by interpolating over log ($\rho$). These values are also consistent with the units used to represent the oxygen concentration.

d) Solution strategy. The calculations were made using finite difference approximations. The columns and rebar were represented on a three dimensional grid system, with a grid spacing of 0.9 cm in all directions. The selected grid size is a compromise between a proper representation of the column including rebar position and size, and the number of computations required to obtain a solution. Larger grid spacing has been use in previous models with satisfactory results [19,20]. The No. 7 rebar was simulated by a square section 1.8 cm per side, which resulted from combining 4 square grid elements. The Jacobi [22] iterative method was used to obtain the numerical solutions.

e) Model outputs. The immediate model outputs are the concentration of oxygen and potential everywhere in the concrete. The following information was extracted from the immediate outputs:

- The current delivered by the anode to each rebar segment, (Sum of the current values corresponding to each discrete element forming the segment)

- The potential of each rebar segment, (Average of the potential values corresponding to each discrete element forming the segment)
- The polarization at each rebar segment (Segment potential before, minus segment potential after CPrev application).

**3-D Model Results vs. Experimental Values**

Figure 8 shows a comparison of the computed and experimentally determined potential of the rebar segments at different elevations. Figure 9 shows a comparison of the computed and experimental polarization of the rebar segments in each column set as function of elevation. In both cases, reasonable agreement between the experimental measurements and computational model was observed.

Figure 10 shows the calculated and measured cathodic current density delivered by the anode to each of the rebar segments. The calculated current density delivered to each segment and trends with elevation compared well with the measured behavior in most instances. However, it is important to note that in the few cases where a larger relative difference in current density occurred, the measured current densities were very small (e.g. upper segments of Set D, experimental current density < 0.001 $\mu A/cm^2$).

**1-D Model Description and Implementation**

A simpler 1-D model was developed, that retained most of the properties of the 3-D model, but requiring a small fraction of the computational resources. This 1-D model is a modified version of one developed previously [23], implemented for conditions similar to those modeled with the detailed 3-D model. A major difference between both models was that the 1-D model did not include provisions for oxygen transport.

A brief description of the 1-D model is as follows. The column was assumed to consist of a stack of discrete steel segments in concrete, all segments considered to be net cathodes. A constant potential source simulated the Zn anode. Figure 11 shows an idealized column with interconnected segments and the corresponding large-signal electrical equivalent circuit, for the case where segments 1 to 9 (or 8 if from set W) are net cathodes. $Rc_i$ is the effective concrete resistance between consecutive rebar segments j and j+1. $Is_j$ is the current associated with rebar segment j. $E_1$ to $E_9$ (or $E_8$) are current-dependent voltage sources representing the potential difference across the metal-concrete interface of the corresponding regions. All segments were considered to be subject only to activation polarization, so that for rebar segment j:

$$E_j = E_{OC} + \beta_C \log \frac{\left|Is_j\right| - I_p}{I_{OC}} \qquad (6)$$

where $\beta_c$ is the Tafel slope for the cathodic reaction, the passive current $I_p$ was used as a constraint to bound the results to the observed OCP, and $I_{OC}$ is the exchange current for the cathodic reactions at the equilibrium potential $E_{OC}$. The polarization parameter values were as in the 3-D model. Since all cathodic rebar segments within a column have the same amount of effective surface area $A_C$, then $I_{0C}=i_{0C}*(A_C)$, similarly $I_p=i_p*(A_C)$.

The effective resistance of the concrete joining consecutive segments j and j+1 was approximated by $Rc_j = \rho_j * d / A_{CS}$, where $\rho_j$ is the measured resistivity of the concrete between the two segments, $A_{CS}$ is the cross-sectional area of the column expressed in $cm^2$, and d is the vertical distance between segments.

Independent equations were formulated, establishing a zero-potential sum for each of the 9 (or 8 if set W) closed loops in the ladder circuit in Figure 11. An additional equation was provided by the requirement that the sum of all the cathodic currents needs to be equal to current of the anode. The resulting system of 10 (or 9) equations was solved numerically to obtain the 10 (or 9) values of Is, using as input the resistivity profile of the column, the polarization parameters of the cathodic reaction, and the Zn anode potential.

The results from both models were in reasonable agreement for comparable calculations, as presented in Figure 12, which reproduces Figure 9 but with the addition of the 1-D model results. The major discrepancy between the 1-D model and the 3-D model is at the lower segment of Set D, as expected since this segment is likely under partial concentration control. These results suggest that the simple 1-D model can be used to do exploratory calculations of field size structures for the portion above high tide (little oxygen diffusional limitation) at a fraction of the computational time needed by the more detailed 3-D model.

**Estimation of the Throwing Power on Field Size Structures using 1-D Model.**

Having established reasonable confidence in the 1-D model, modifications to represent cases replicating field size structures were implemented. The throwing power on field size structures provided by a Zn bulk anode was quantified with this 1-D model to evaluate the applicability of this approach to obtain CPrev. The model calculations focus on the portion above high tide where little oxygen diffusional limitation is expected.

**Assumptions Made to Represent Field Size Structures.**

Columns of two different lengths were modeled: one was 5 m long, typical of field size structures and the other 120 m simulating an infinite length limiting case for conservative evaluation. The column, of selectable diameter $\phi_{col}$, was divided into a stack of discrete elements. Fourty-eight segments were used with a segmented thickness dx =0.104 m to discretize the 5 m column. The first 1.25 m of the 120 m column were divided into slices of thickness of dx=0.104 m, above this coarser segments were used. Figure 13 shows how the columns were discretized and also the corresponding equivalent circuit.

The current and potential distribution in the column was modeled by assuming a constant anodic passive current ($i_p = 2.5x10^{-9}$ A/$cm^2$ as in the experiment or $i_p = 1.x10^{-8}$ A/$cm^2$ as a more conservative value [24]), accounting for the polarization behavior of the cathodic reaction, and for simplicity a constant electrical resistivity ($\rho$) of the intervening concrete. When calculating the $I_{OC}$ and $I_p$ (per Eq. (6)) of each slice, appropriate account was made for the steel surface area of that slice.

The resistance of each slice was $R_j = dx_j * \rho / A_c$, where $A_c$ is the column cross-section area ($\pi\phi_{col}^2/4$) and $dx_j$ is the length of slice j. The current is proportional to the steel area ($A_s$) per unit length. The ratio of $A_s$ to the external surface area per unit length of the concrete ($A_{con}$) is

termed the steel factor (SF). In typical marine substructures applications SF is often in the order of unity [25].

Either $\beta_c$=145 mV/decade (similar to the value derived from Figure 5) or $\beta_c$=100 mV/decade (as a more conservative alternative) were used as parameters. $i_{OC}= 2.5x10^{-11}$ A/cm$^2$ was used in combination with appropriate $E_{OC}$ values from 235 mV to 113 mV so as to have an open circuit potential of ~–100 mV, representative of typical passive steel values observed when CPrev is not in place.

The presence of the Zn anode was simulated by connecting a constant potential source (-1 V in this case) beneath the lowest column slice component. The appropriate intervening concrete resistance between the lower slice and the anode was used. Similarly to the 1-D modeling of the laboratory columns appropriate equations were written and solved numerically. From the calculated polarization values, the elevation in the column where the polarization reached 100 mV or 200 mV was determined and designated as the throwing power $h_{throw}$ for that polarization level. The 100 mV was chosen because, as indicated in the introduction, a substantial increase in the chloride threshold has been reported for that polarization level. The 200 mV value explores a more conservative condition.

**1-D Model Field Size Structures. Results and Discussion.**

For a given column length and polarization level, the value of $h_{throw}$ depends on the values of $\rho$, $\phi_{col}$ and SF. The equivalent circuit in Figure 13.b is that of a uniform transmission line [26], which permits combining these three parameters into a single normalizing parameter: $P= SF\rho/\phi_{col}$, having the dimension of resistance ($\Omega$). This parameter was used in the generation of the performance curves shown in Figures 14 and 15. In these figures the dotted lines correspond to columns 5 m long, and the continuous lines to unlimited height columns. The $i_p$ and $\beta_c$ value choices discussed above were used.

The significance of the results presented in Figure 14 may be understood by considering the case of a tall substructure column of typical size and steel density, for example $\phi_{col}$ =100 cm and SF=1. When the concrete resistivity is 10 k$\Omega$ cm (a value typical of medium quality concrete [27-29]) P is equal to 100 $\Omega$, in the middle of the x axis. For such case and with steel having polarization characteristics similar to those encountered in the laboratory columns ($\beta_c$=145 mV/decade, $i_p = 2.5\ 10^{-9}$ A/cm$^2$), $h_{throw}$ was approximately 2 m. This projection indicates that cathodic prevention (polarization > 100 mV in Figure 14) by a submerged zinc anode may be achieved under these conditions typical of much of the tidal and splash evaporation zone. However, if all else were to remain the same but $\rho$ was instead 100 k $\Omega$–cm (e.g. very low permeability concrete, or drier overall conditions than in the previous case), $h_{throw}$ would become only ~ 1m and the >100 mV prevention levels would be limited to the lower splash zone. If the cathodic reaction were less polarizable than assumed above, for example having $\beta_c$ = 100 mV/decade and $i_p = 10^{-8}$ A/cm$^2$, $h_{throw}$ would become only ~0.5 m or ~0.3 m for the 10 k $\Omega$–cm or 100 k $\Omega$–cm cases respectively. Again, under these circumstances polarization levels > 100 mV would be achieved only in a fraction of the lower splash zone. Intermediate cases can be evaluated by reference to the appropriate curves. Except for combinations of highly conductive concrete with large column diameter / low steel density, the 5 m long columns behaved similar to the unlimited height cases. It should be noted that

polarization may reach further than indicated in Figure 14 if significant concentration polarization were to exist at the lower elevations.

Figure 15 shows curves for polarization levels > 200 mV. For P equal to 100 Ω (as in the previous paragraph) and with steel having polarization characteristics similar to those encountered in the laboratory columns, $h_{throw}$ ~0.8 m, protecting only the lower splash zone. This distance is only 40 % of the distance observed when considering 100 mV polarization. With ρ equal to 100 kΩ-cm and all else the same, $h_{throw}$ becomes only 0.3 m and only a portion of the lower splash zone would be protected. If the cathodic reaction were less polarizable, for example having $\beta_c$ = 100 mV/decade and $i_p = 10^{-8}$ A/cm$^2$, $h_{throw}$ would become only ~0.23 m or ~0.12 m for the 10 k Ω–cm or 100 k Ω–cm cases respectively. Under these circumstances polarization levels > 200 mV would be marginal and achieved only in a small fraction of the lower splash zone.

The estimates obtained with the 1-D model adapted to field size structures suggest that with an immersed anode potentially useful levels of cathodic prevention may be reasonably expected, even under conservative assumptions, in the area immediately above high tide where conditions are otherwise very severe. The use of sacrificial CPrev anodes then appears to be promising in controlling corrosion in a region where early damage is often observed. These estimates suggest also that Cprev implemented using bulk anodes may not be effective at higher elevations unless a favorable combination of system dimensions and electrochemical properties is present. A more pessimistic overall outlook results if at least 200 mV polarization is needed for adequate CPrev. Further testing should be conducted to reduce uncertainty in the expected range of concrete and steel polarization properties. Such information would allow removing some conservatism in the projections and refine the prognosis for CPrev at higher elevations on substructural elements.

The 1-D model used to evaluate CPrev application could be easily adapted in future work to evaluate the ability of immersed anodes to provide conventional cathodic prevention to substructural elements with small anodic regions, as may be present where preexisting cracks intersect rebar. Another alternative future application could address similar implementation of CPrev to substructural elements with epoxy coated rebar with various levels of coating distress.

## CONCLUSIONS

1) CPrev using sacrificial zinc bulk anodes was investigated on aged laboratory columns simulating partially submerged piles. It was observed that rebar segments receiving a current density >0.01 μA/cm$^2$ were polarized by >100 mV.

2) The 3-D model and the 1-D model simulations were compared with the experimental results. Both models successfully represented the reduction in throwing power resulting from an increase in concrete resistivity. The results of both models were generally similar to the measured values except that the 1-D model (which did not include combined cathodic polarization provisions) did not match well the behavior of a segment low in the column subject to partial oxygen concentration polarization. Since the 1-D model required a fraction of the computational time of the 3-D model, the 1-D model was used for exploratory calculations of field size structures for the portion above high tide

3) The estimates obtained with the 1-D model adapted to field size structures suggest that with an immersed anode polarization > 100 mV may be reasonably expected, even under conservative assumptions, in the area immediately above high tide where conditions are otherwise very severe. These estimates suggest also that Cprev implemented using bulk anodes may not be effective at higher elevations unless a favorable combination of system dimensions and electrochemical properties is present.

4) The 1-D model used to evaluate CPrev application could be easily adapted in future work to evaluate the ability of immersed anodes to provide conventional cathodic prevention to substructural elements with small anodic regions, as may be present where preexisting cracks intersect rebar.

## Acknowledgements

The authors acknowledge the support of the Florida Department of Transportation and Engineering Computing Services of the University of South Florida. The findings and opinions are those of the authors and not necessarily those of the supporting organizations. One of the authors (F.J.P.) acknowledges the scholarship provided by the National Council for Science and Technology (CONACYT-México)

## References

1 P. Pedeferri, Construction and Building Materials, 10, 5(1996): p. 391-402
2 L. Bertolini, F. Bolzoni, L. Lazzari, T. Pastore and P. Pedeferri, Journal of Applied Electrochemistry, 28, 12(1998): p. 1321-1331
3 L. Bertolini, F. Bolzoni, L. Lazzari, and P. Pedeferri, “Applications of Cathodic Protection to Steel in Concrete”, Internationale Zeitschrift für Bauinstandsetzen und Baudenkmalpflege, V 6, (2000): p.655-668
4 S.F. Daily, K. Kendell, Materials Performance 37, 10(1998): p.19-25
5 M. Tettamanti, A. Rossini, and A. Cheatani, Materials Performance 36, 9(1997): p.21-25
6 L. Manian, M. Surkein, Materials Performance 38, 5(1999): p. 30-35
7 C.L. Page, G. Sergi, Journal of Materials in Civil Engineering 12, 1(2000), p.8-15
8 Alonso C., Andrade C., Castellote M., “The Influence of the Electrical Potential in the Chloride Threshold for Rebar Depassivation”, In *Proc. 10th International Congress on the Chemistry of Cement*, vol 4, H. Justnes, ed., Gothenburg, Sweden, Paper No. 4iv082 (1997)
9 Alonso C., Castellote M., Andrade C., “Dependance of Chloride Threshold with the Electrical Potential of Reinforcements”, In *Second International RILEM Workshop on Testing and Modeling the Chloride Ingress into Concrete*, PRO 19, RILEM Publications, Cachan France, 415-428 (2000)
10 Arup H., , “A New Method for Determining Chloride Thresholds as a Function of Potential in Field Exposure Tests”, In *Durability of Concrete in Saline Environment*, Cementa AB, Lund, Sweden, 107-112 (1996)
11 Sandberg P., “The effect of defects at the steel – concrete interface, exposure regime and cement type on pitting corrosion in concrete”, Report TVBM-3081, Lund, Sweden, (1998)
12 Sandberg P., “Chloride initiated reinforcement corrosion in marine concrete”, Report TVBM-1015, Lund, Sweden, (1998)
13 A.A. Sagüés, M.A. Pech-Canul, A.K.M. Al-Mansur, “Corrosion Macrocell Behavior of Reinforcing Steel in Partially Submerged Concrete Columns”, submitted to publication (2000).
14 Castro, P., Sagüés, A.A., Moreno, E.I., Maldonado, L. and Genescá J., Corrosion 52, 8(1996): 609-617
15 F.J. Presuel, A. A. Sagüés, S.C. Kranc, “Steel Activation in Concrete Following Interruption of Long Term Cathodic Polarization”, presented at CORROSION/2002, paper02259 (Houston, TX: NACE International, 2002)
16 C.L. Page in Corrosion of Steel in Concrete, Report of the Technical Committee 60-SCS, Editor P. Schiessl, (1988): p 17
17 J.P. Bromfield, Corrosion of Steel in Concrete, (London, E&FN Spon, 1997)
18 F. Pruckner , “Corrosion and Protection of Reinforcement in Concrete Measurements and interpretation”, Ph.D. Dissertation, University of Vienna. (2001)

19 S.C. Kranc, A.A. Sagüés, F.J. Presuel-Moreno, “Computational and Experimental Investigation of Cathodic Protection Distribution in Reinforced Concrete Marine Piling”, presented at CORROSION/1997, paper No.231, (Houston, TX: NACE International, 1997)
20 C. Kranc, A.A. Sagüés, Corrosion Science. 43, 7(2001): 1355-1372
21 CRC. Handbook of Chemistry and Physics, R.C. Weast Editor, CRC Press, Cleveland, (1973).
22 R. Burden, J. Faires, Numerical Analysis, (Boston, PWS-KENT Pub, 1985), p.402-403
23 A.A. Sagüés, H.M. Perez-Duran, R.G. Powers, Corrosion 47, 11(1991): p. 884-893.
24 Li, L.; Sagüés, A., “Effect Of Metal Surface Condition On The Chloride Corrosion Threshold Of Reinforcing Steel In Alkaline Solutions”, presented at CORROSION/2000, paper 801 (Houston, TX: NACE International, 2000)
25 A.A. Sagüés, R.G. Powers, Corrosion 52, 7(1996): p. 508-522
26 S. Goldman, Transformation Calculus and Electrical Transients, (New York, Prentice-Hall, 1949): p.285-315
27 S. Feliu, J.A. Gonzalez, and C. Andrade, “Electrochemical methods for on-site determination of corrosion rates of rebars”, Techniques to asses the corrosion activity of steel reinforced concrete structures, ASTM STP 1276, N. Berke, E. Escalante, C Nmai, and D Whiting, eds, ASTM, West Conshohocken, Pa., p.107-118 (1996). Resistivity Concrete quality Ref.
28 R. Polder, Construction and Building Materials 15, 2-3(2001): p.125-131
29 C. Andrade, C. Alonso, Construction and Building Materials 15 2-3(2001) p.141-145

Table 1. Average polarization (mV) of each rebar segment for each of the 4 columns and grouped by column set.

| Segment | W1 | W2 | Average Set W | D1 | D2 | Average Set D |
|---|---|---|---|---|---|---|
| 1 | 125 | 116 | 121 | 25 | 27 | 26 |
| 2 | 130 | 130 | 130 | 26 | 29 | 28 |
| 3 | 142 | 140 | 141 | 35 | 36 | 36 |
| 4 | 163 | 160 | 161 | 47 | 47 | 47 |
| 5 | 199 | 195 | 197 | 73 | 70 | 72 |
| 6 | 265 | 252 | 259 | 137 | 129 | 133 |
| 7 | 382 | 366 | 374 | 259 | 280 | 270 |
| 8 | 525 | 513 | 519 | 363 | 383 | 373 |
| 9 | | | | 717 | 716 | 716 |

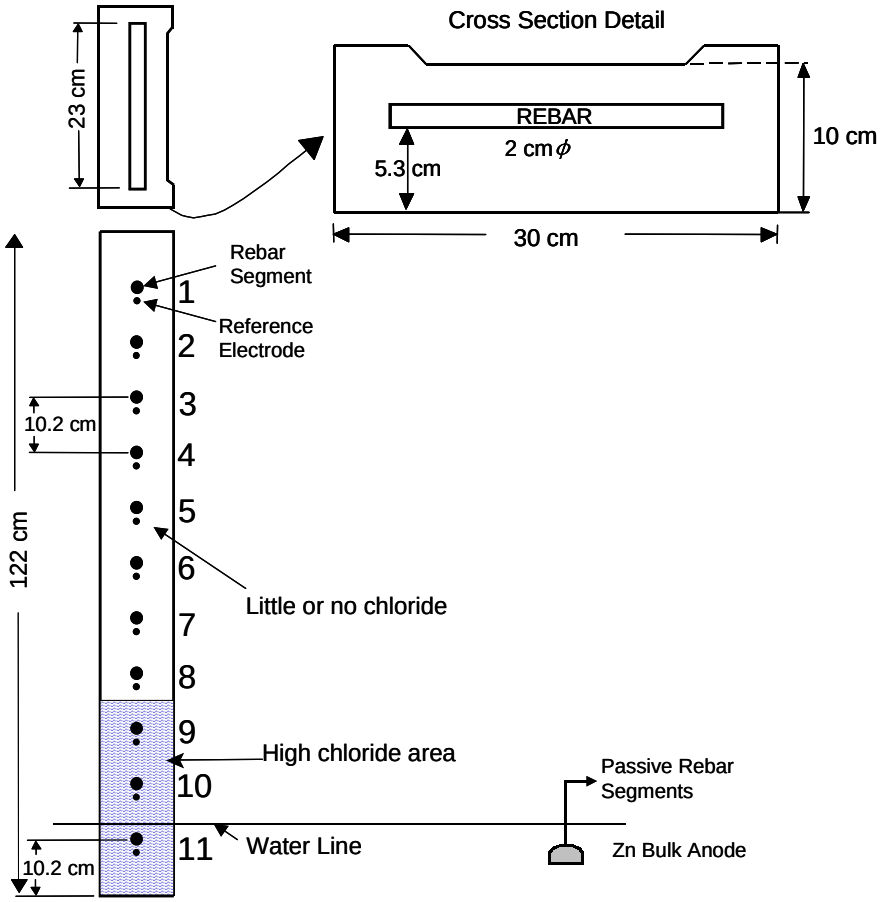


Figure 1. Column configuration.

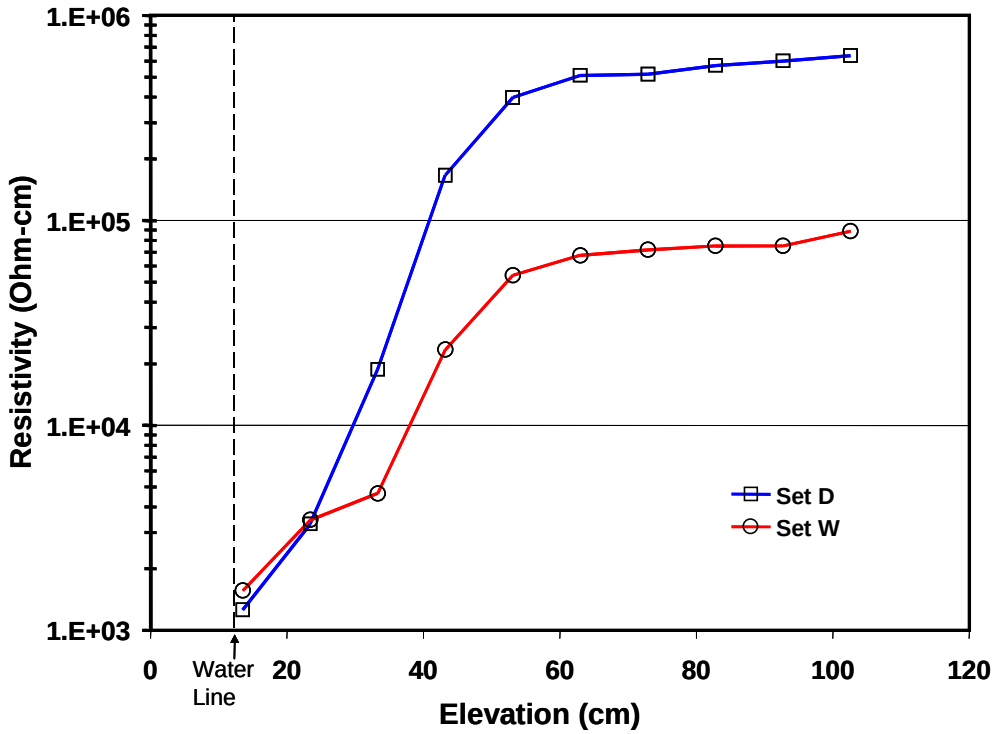


Figure 2. Resistivities measured 7 days before connecting the anodes. Average of each set.

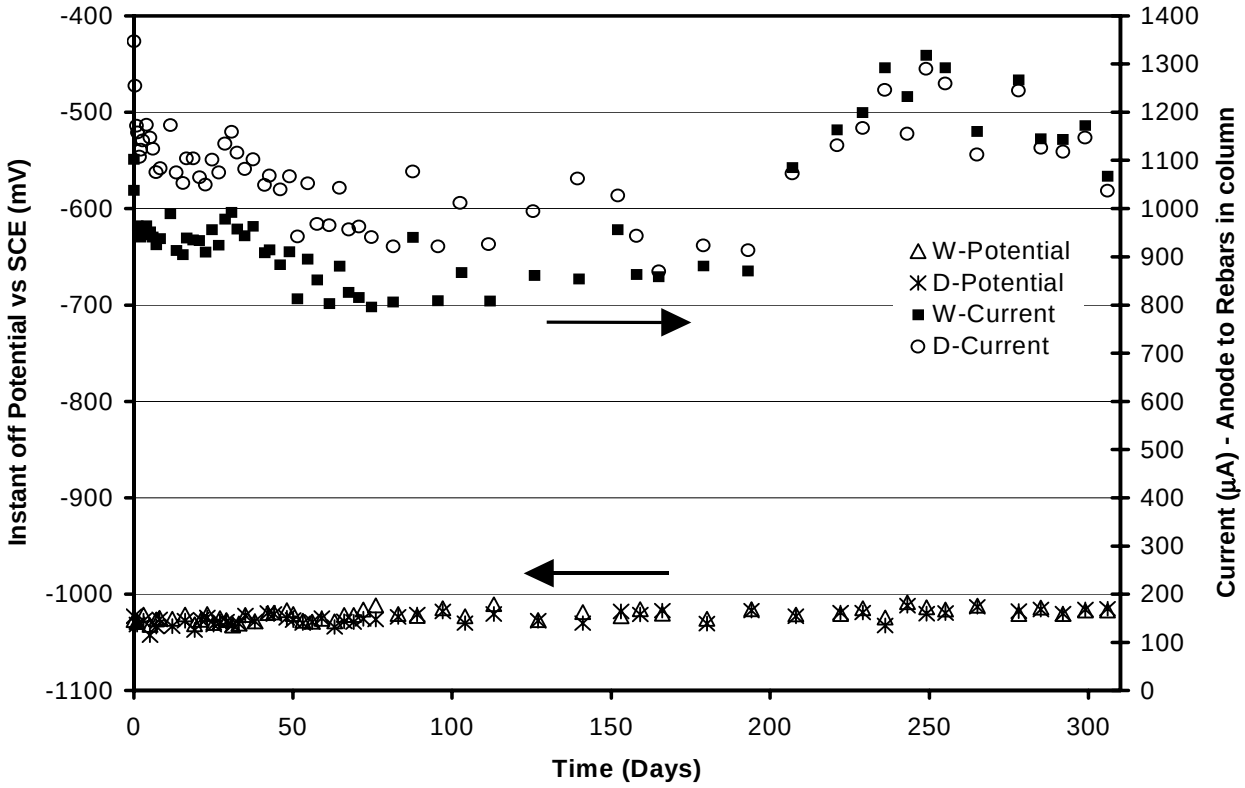


Figure 3. Zn anode instant off potential and current delivered to the rebar group, averaged by column set during CPrev application.

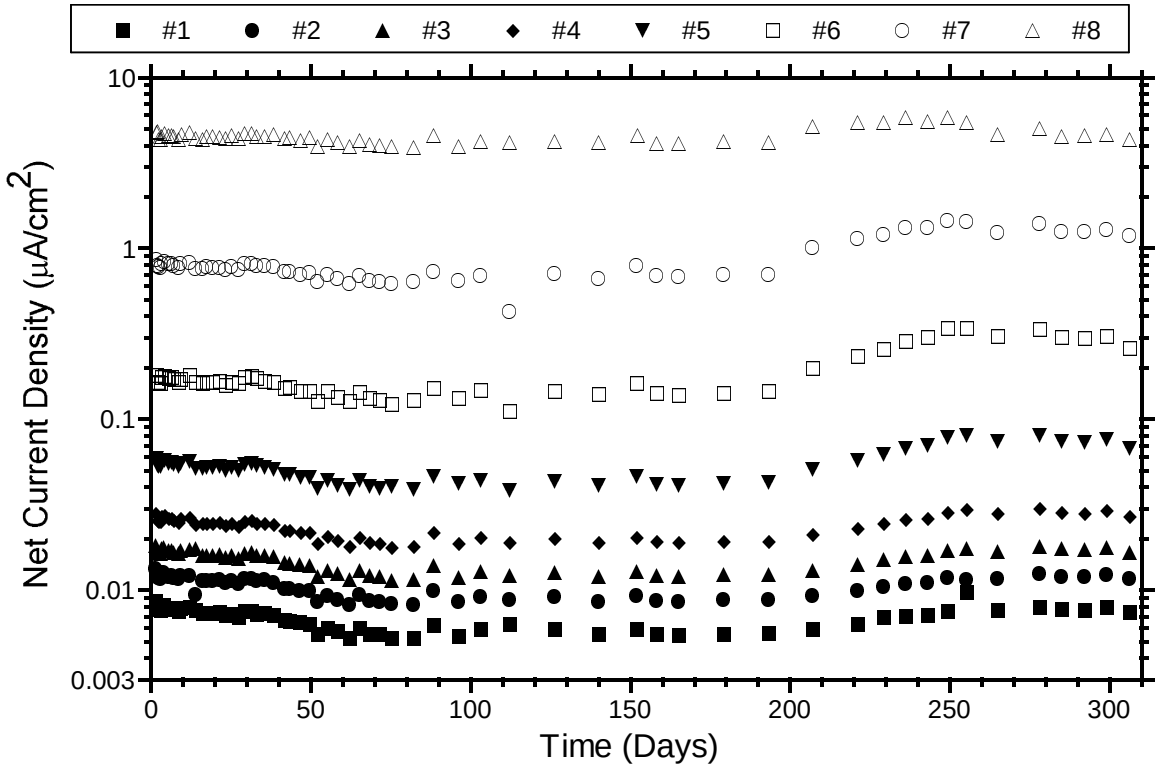


Figure 4. Applied cathodic current densities measured for each rebar segment in column W1 during CPrev application (after the first day).

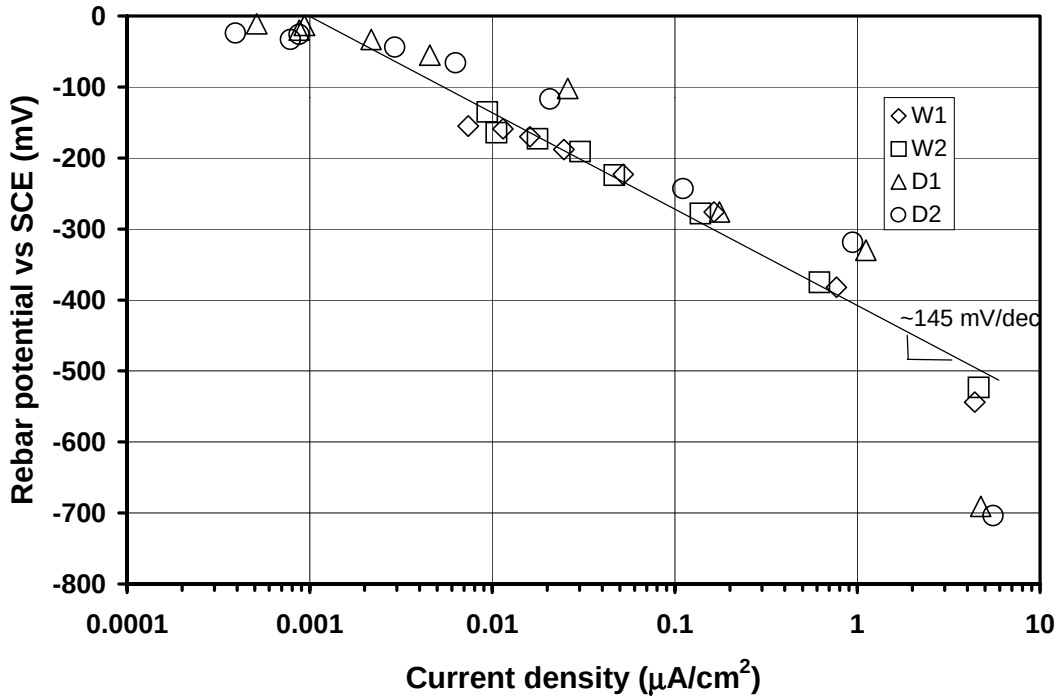


Figure 5. Potential vs current density associated with each rebar segment after applying cathodic prevention for 80 days.

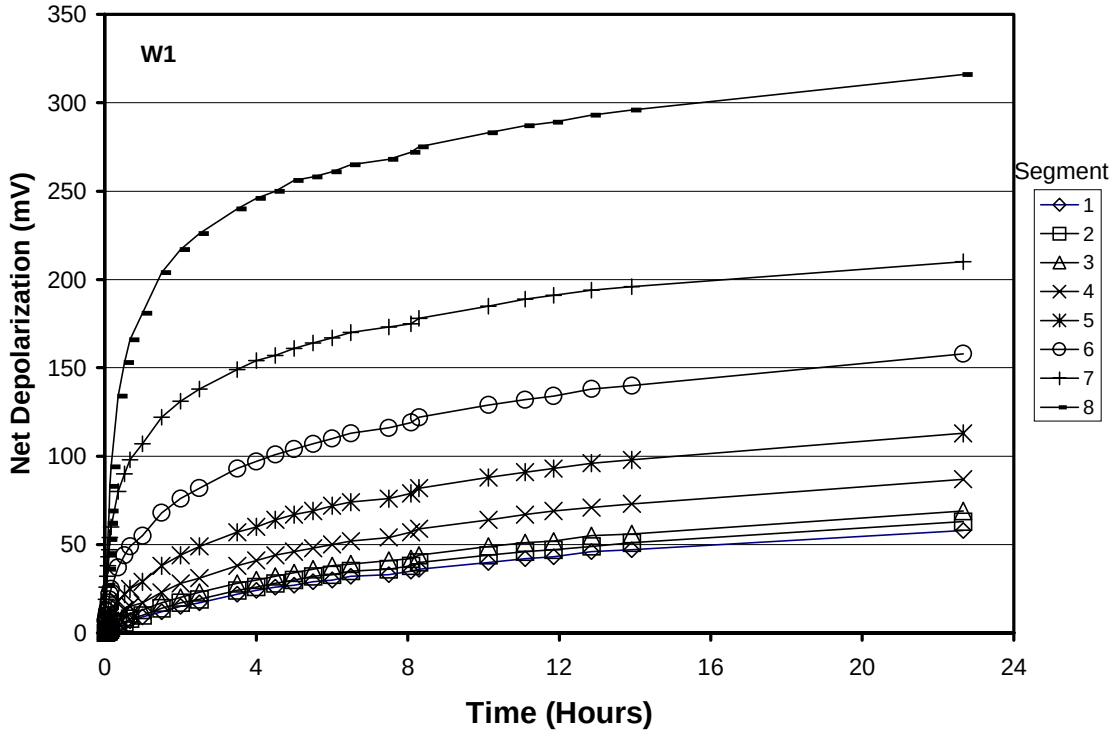


Figure 6. Net depolarization measured for rebar segments of column W1.

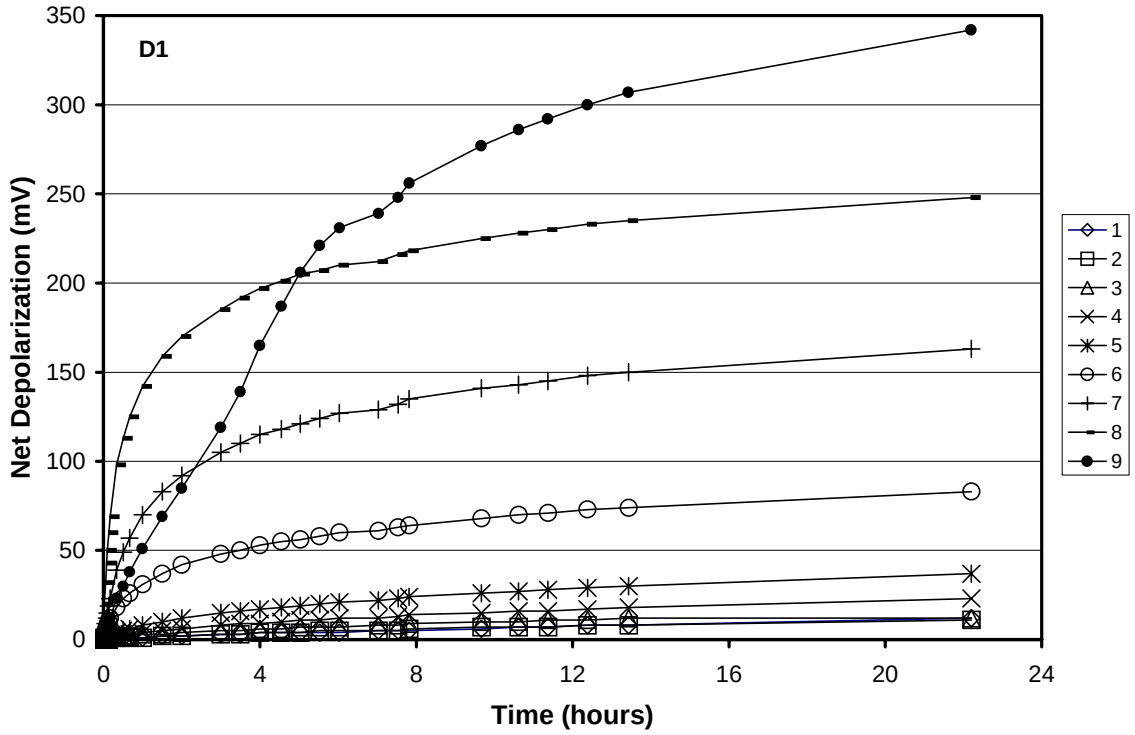


Figure 7. Net depolarization measured for rebar segments of column D1

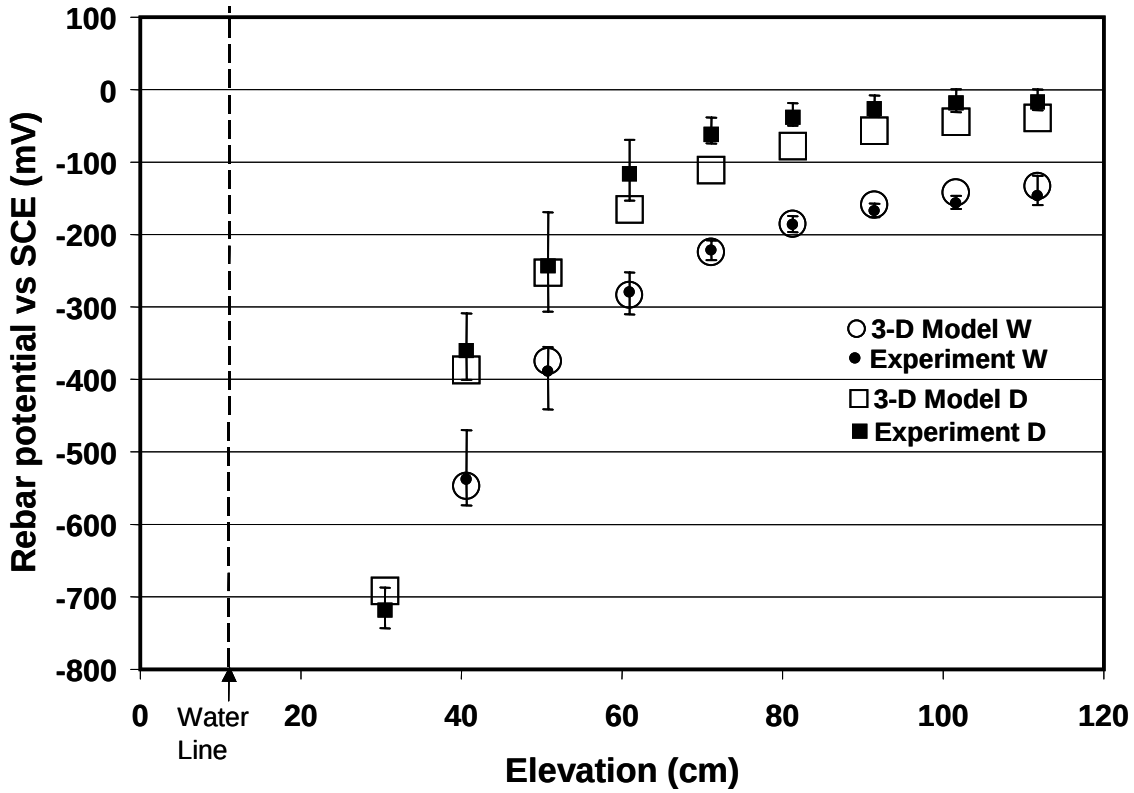


Figure 8. Rebar segment potentials after the Zn anode was connected, comparison of 3-D model and experimental results.

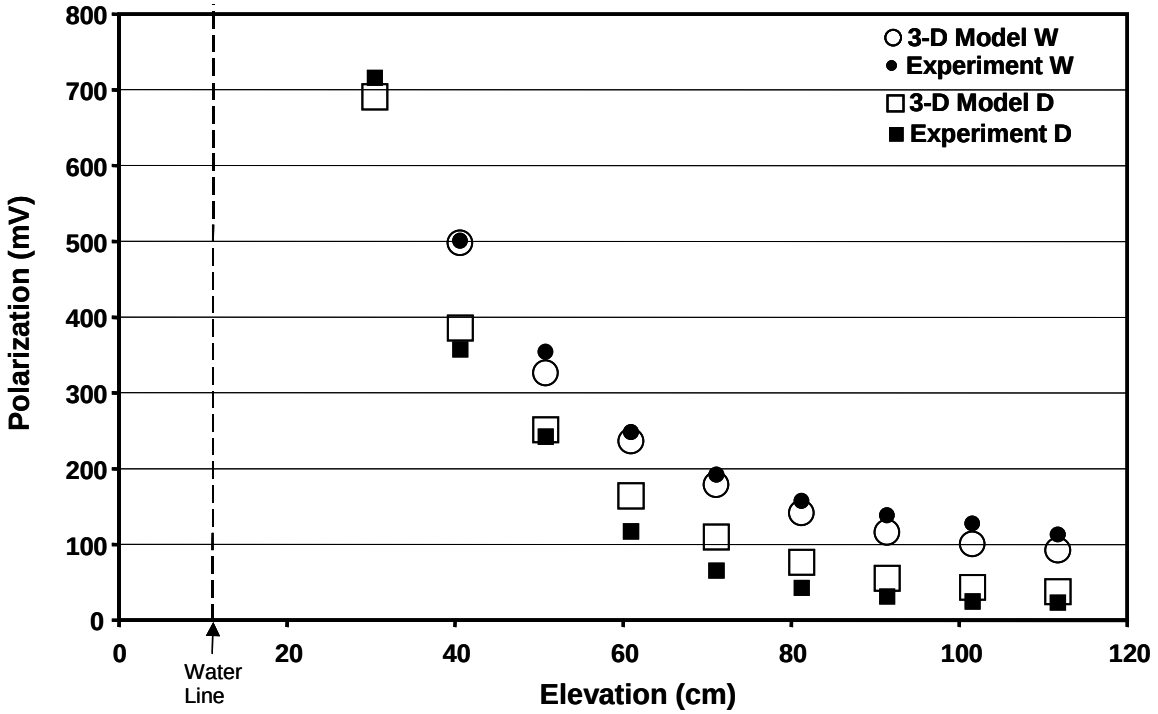


Figure 9. Polarization observed at each rebar segment for both column types, comparison of 3-D model and experimental results.

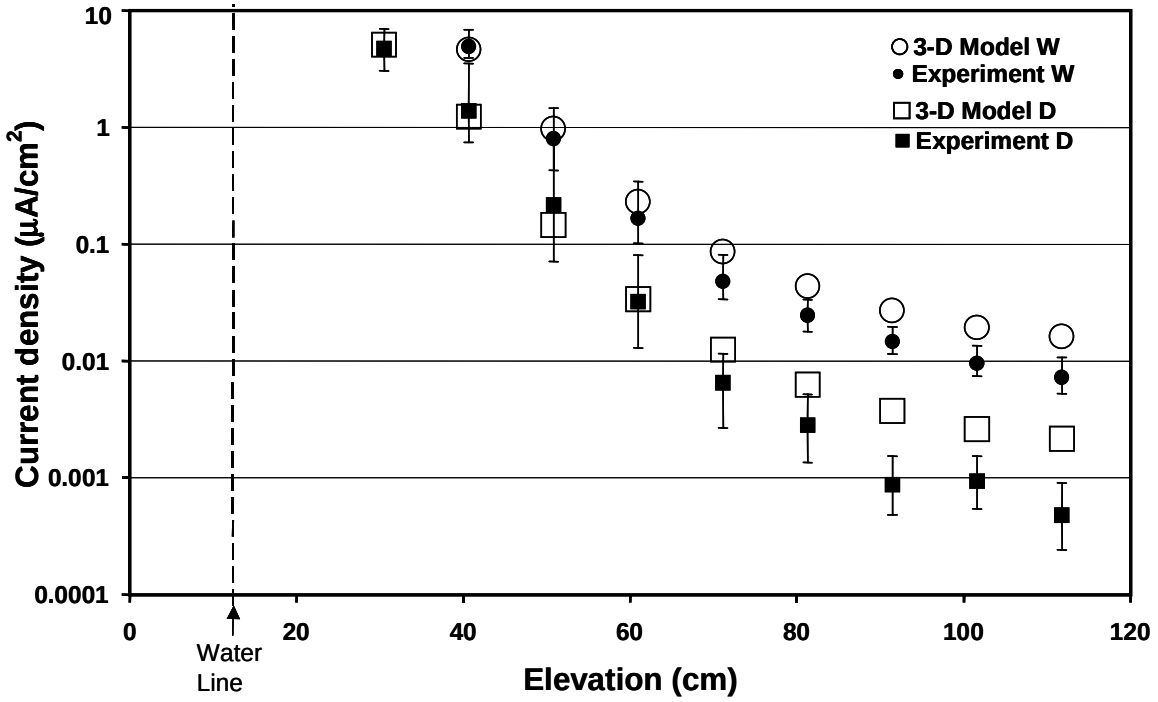


Figure 10. Current density delivered by the anode to each rebar segment, comparison of 3-D model and experimental results. Experimental results show the range and average current density values measured for each rebar segment (grouped per column set).

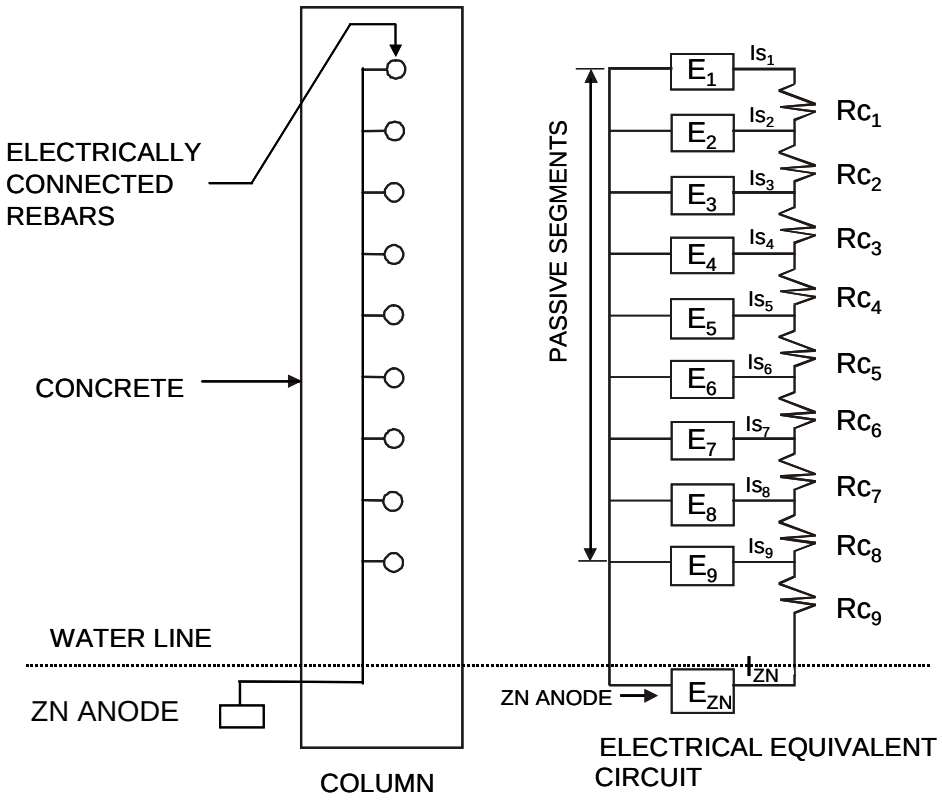


Figure 11. Schematic of electrical equivalent for 1-D model.

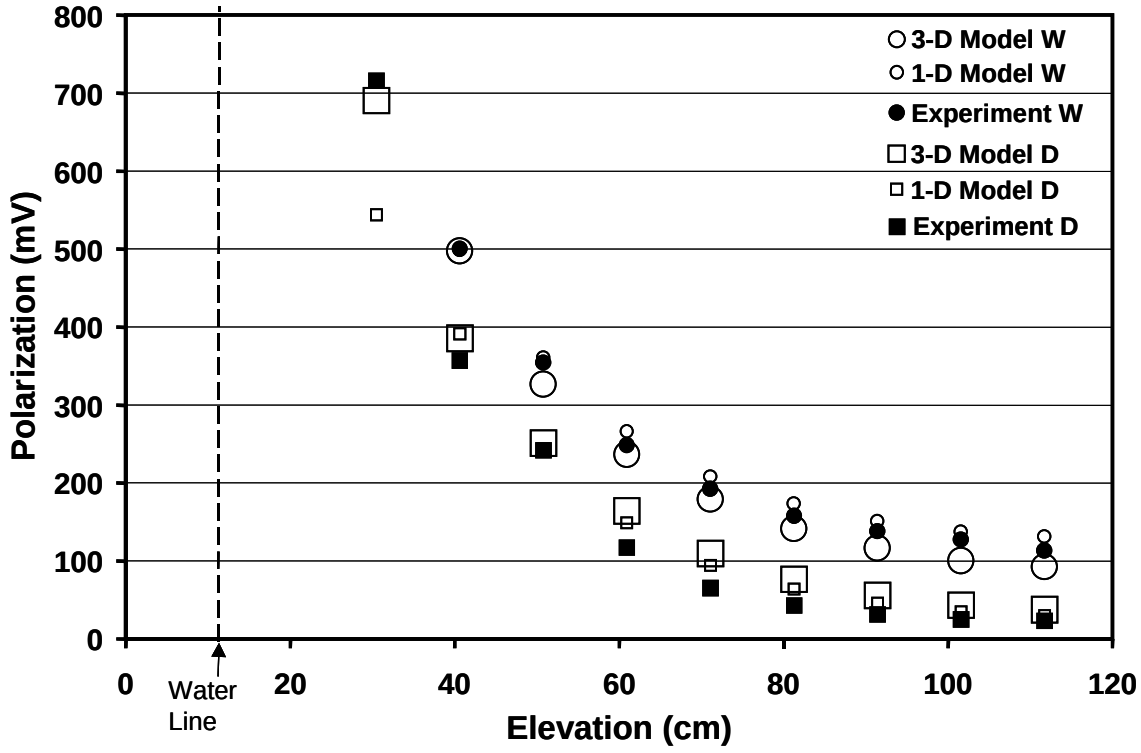


Figure 12. Comparison of the polarization obtained with 1-D model, 3-D model and the experimental results, for both column sets.

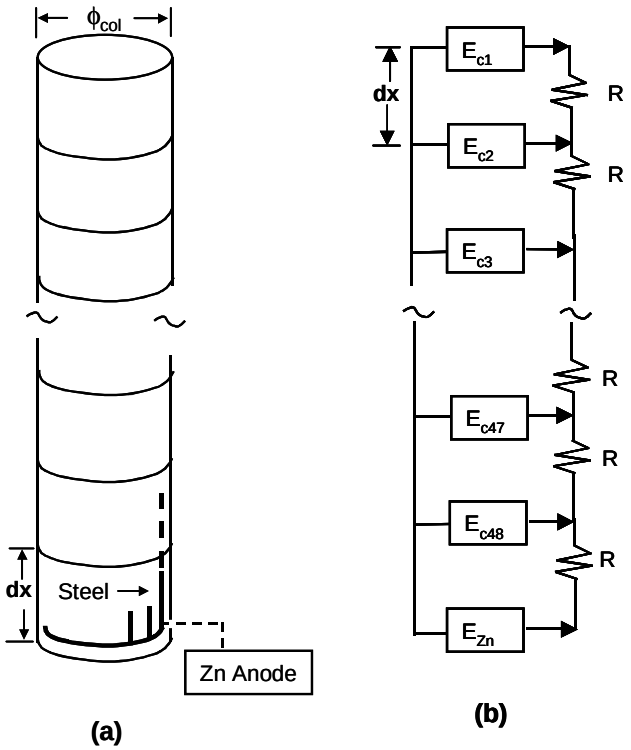


Figure 13. a) Column discretization, b) Equivalent Circuit

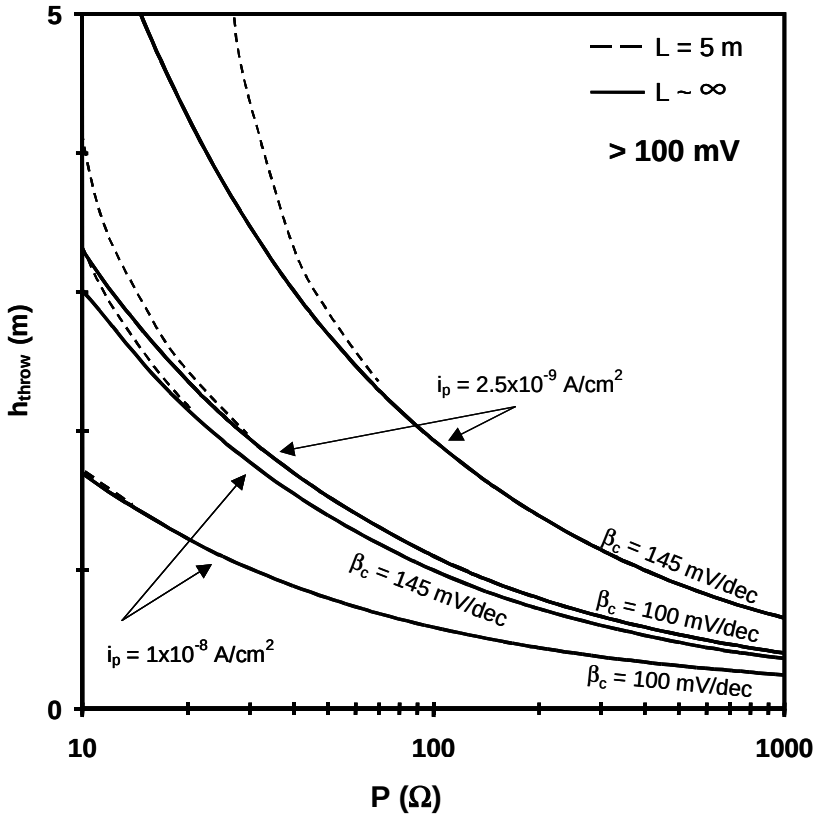


Figure 14. Performance curves derived from the 1-D model for 5 m and ~∞ long columns, for polarizations > 100 mV.

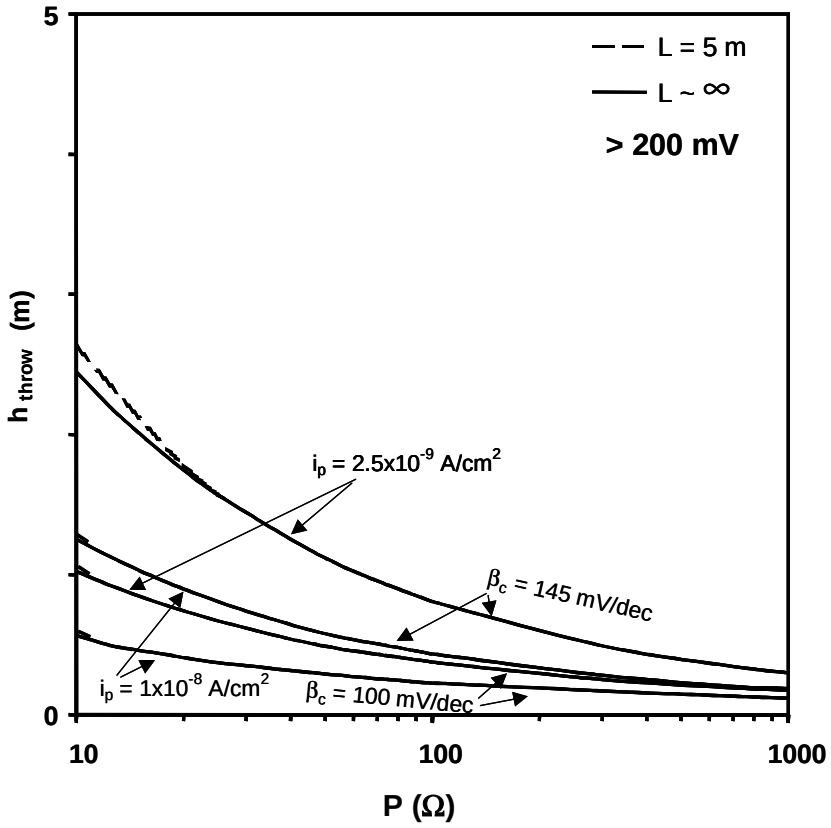


Figure 15. Performance curves derived from the 1-D model for 5 m and ~∞ long columns, for polarizations > 200 mV.